PHYSICAL REVIEW B **89**, 235319 (2014)

Layer-controlled band gap and anisotropic excitons in few-layer black phosphorus

Vy Tran, Ryan Soklaski, Yufeng Liang, and Li Yang
Department of Physics, Washington University in St. Louis, St. Louis, Missouri 63136, USA
(Received 17 February 2014; revised manuscript received 4 June 2014; published 26 June 2014)

We report the quasiparticle band gap, excitons, and highly anisotropic optical responses of few-layer black phosphorous (phosphorene). It is shown that these materials exhibit unique many-electron effects; the electronic structures are dispersive essentially along one dimension, leading to particularly enhanced self-energy corrections and excitonic effects. Additionally, within a wide energy range, including infrared light and part of visible light, few-layer black phosphorous absorbs light polarized along the structures' armchair direction and is transparent to light polarized along the zigzag direction, making them potentially viable linear polarizers for applications. Finally, the number of phosphorene layers included in the stack controls the material's band gap, optical absorption spectrum, and anisotropic polarization energy window across a wide range.

DOI: 10.1103/PhysRevB.89.235319 PACS number(s): 71.35.Cc, 31.15.A−, 73.22.−f, 78.20.Ci

I. INTRODUCTION

It is difficult to overstate the interest in graphene and graphene-inspired two-dimensional (2D) crystals [1–3]. Recently, an attractive finite-gapped 2D semiconductor, few-layer black phosphorus (phosphorene), was successfully fabricated [4–7]. Despite phosphorene's promising direct band gap, one cannot realistically envision phosphorene devices until its fundamental excited-state properties, such as its quasiparticle (QP) band gap and optical spectrum, are obtained. No such experimental measurements have been made, thus corresponding first-principles predictions are indispensable. Furthermore, these excited-state quantities are known to be dictated by many-electron effects, e.g., electron-electron (*e*-*e*) and electron-hole (*e*-*h*) interactions. Therefore, it is essential to turn to *ab initio* calculations that incorporate many-body self-energy corrections and excitonic effects to advance the forefront of phosphorene research and its applications.

In addition to its direct band gap, few-layer black phosphorus may exhibit unique excitonic effects that have not been observed in other 2D structures. For example, recent experiments have observed a strongly anisotropic conducting behavior [5]. It is of particular interest to investigate the effect that this anisotropy has on exciton formation and thus on the optical properties of this material. Van der Waals (vdW) interactions allow layers of phosphorene to be stacked; the band gap of the resulting material depends on the number of stacked layers (N) [5,8]. This has been observed in other 2D semiconductors [9–11]. Because the band gap is a fundamental factor in determining electronic screening and corresponding many-electron interactions in the material, the optical spectra and excitonic effects of few-layer phosphorene shall also be controlled by the number of stacking layers. Therefore, studying few-layer phosphorene provides a chance to observe how the electronic structure and excitonic properties of a 2D material transition to that of a 3D material.

In this paper, we perform first-principles GW-Bethe-Salpeter equation (BSE) simulations to study the QP band gap and optical spectra of few-layer and bulk black phosphorous, resulting in several important findings. First, we observe significant many-electron effects. For monolayer phosphorene, the self-energy correction enlarges the band gap from 0.8 eV to 2 eV, and the lowest-energy optical absorption peak is reduced to 1.2 eV because of a huge exciton binding energy (around 800 meV). These strong many-electron effects result from unique quasi-one-dimensional (1D) band dispersions of phosphorene. Second, we observe highly anisotropic optical responses. Few-layer black phosphorous strongly absorbs light polarized along its lattice's armchair direction, but it is transparent to light polarized along the zigzag direction. It is chiefly absorbent across the infrared-light range and part of the visible-light range, making it an ideal candidate for use as an optical linear polarizer with a wide energy window. Finally, the band gap, exciton binding energies, optical absorption spectrum, and linear polarization energy window of phosphorene can all be broadly tuned by changing the number of stacked layers. This serves as a convenient and efficient method for engineering the material's excited-state properties.

The remainder of this paper is organized as follows: In Sec. II, we introduce the atomic structures of our calculated few-layer black phosphorus and computing approaches; in Sec. III, QP band gaps and their scaling laws according to stacking layers are presented; in Sec. IV, we show excitonic effects on optical absorption spectra of few-layer black phosphorus; in Sec. V, we present anisotropic optical spectra according to the polarization direction of incident light; in Sec. VI, we show wave functions of typical anisotropic excitons; in Sec. VII, impacts of the interlayer distance on QP band gaps and many-electron interactions are discussed; in Sec. VIII, we summarize our studies and conclusion.

II. ATOMIC STRUCTURES AND COMPUTING APPROACH

The atomistic ball-stick models of few-layer black phosphorus are presented in Figs. 1(a) and 1(b) [12,13]. Their in-plane structures are fully relaxed according to the force and stress calculated by density functional theory (DFT) within the PBE functional [14], while the interlayer distance of few-layer black phosphorus is obtained by the vdW functional. For bulk black phosphorus, we use the available experimentally measured interlayer distance. The ground-state wave functions and eigenvalues are calculated by DFT/PBE with a k-point grid of $14 \times 10 \times 1$ for few-layer structures and $14 \times 10 \times 4$ for bulk structures. All calculations use a plane-wave basis with a 25 Ry energy cutoff with a norm-conserving pseudopotential [15]. The QP energy is calculated by the single-shot G_0W_0

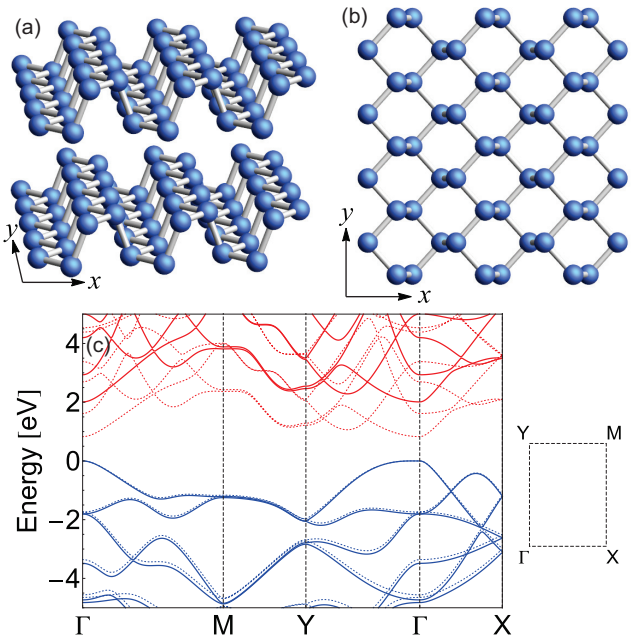

FIG. 1. (Color online) (a) The ball-stick model of few-layer phosphorous. The x axis is perpendicular to and the y direction parallel with the ridge direction, as indicated. (b) Top view of monolayer phosphorene. (c) The DFT-calculated (dashed lines) and GW-calculated (solid lines) band structures of monolayer phosphorous. The top of the valence band is set to be zero.

approximation with the general plasmon pole model [16]. The involved unoccupied band number is about ten times of that of valence bands to achieve the converged dielectric function. The excitonic effects are included by solving the BSE with a finer k-point grid of $56 \times 40 \times 1$ ($35 \times 25 \times 10$ for bulk structures) [17]. A slab Coulomb truncation is crucial to mimic suspended structures [18,19]. Because of the depolarization effect [20,21], only the incident light polarized parallel with the plane structure is considered in studying optical spectra.

III. QP BAND GAP

The DFT and QP band structures of monolayer phosphorene are presented in Fig. 1(b). The band gap is approximately located at the Γ point and the self-energy correction enlarges the band gap from the DFT value of 0.8 eV to 2.0 eV, which is ideal for potentially broad electronic applications [22,23]. The calculated 150% enhancement is substantially larger than in other 2D semiconductors [24–28]. This is due to the highly anisotropic band structure of the lowest conduction band and highest valence band, as shown in Fig. 1(b). In particular, the band dispersion is very flat along the Γ-Y (zigzag) direction with a large effective mass of around 6.2 m_e. This confines particles to an effective 1D environment along the armchair direction, and the effective lower dimension contributes to a larger self-energy correction.

It has to be pointed out that the exact top of the valence band is slightly away from the Γ point. However, the difference between the energy at the Γ point and the actual top of the valence band is less than 10 meV. Therefore, we still approximately regard phosphorene as a direct-band-gap semiconductor.

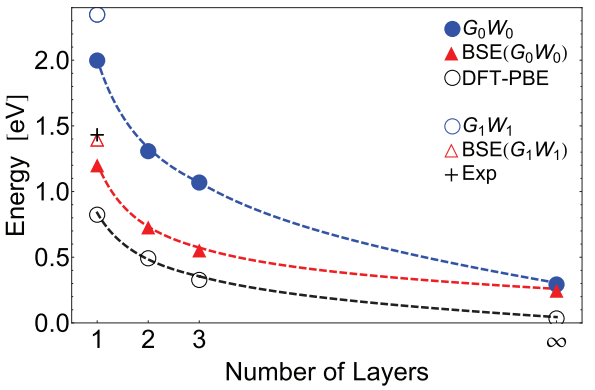

FIG. 2. (Color online) The evolution of band gap calculated by different methods and optical absorption peak according to the stacking layer number of few-layer phosphorene. The power-law fitting curves are presented by dashed lines. The experimental optical peak position is read from Ref. [5].

For multilayer phosphorene, the QP band gap and self-energy corrections vary dramatically according to the stacking layer number, although their band-structure topologies are roughly similar to that of monolayer phosphorene. As shown in Fig. 2, the QP band gap changes from 2 eV (monolayer) to 0.3 eV (bulk). These bounds provide a wide range of tunability for the band gap and corresponding electronic properties. As evidence of the reliability of our simulation, our calculated QP band gap of bulk phosphorous is around 300 meV, which is in excellent agreement with experimental results (0.33 eV) [29,30].

A power law fit of the form $(A/N^{\alpha} + B)$, where N is the number of layers, is applied in Fig. 2, the results of which are reported in Table I. Surprisingly, the GW-calculated band gaps follows the $1/N^{0.7}$ power law, which decays significantly slower than the usual quantum confinement result $(1/N^2)$. This weaker quantum confinement effect results from the vdW interfaces, which partially isolate electrons between neighboring sheets. A simple model illustrated in Fig. 3 shows this effect by mimicking this quantum confinement effect by an infinite quantum well superposed with a series of potential barriers. Figure 3(a) presents the Hartree potential profile obtained by first-principles DFT calculations. The vacuum level is set to be zero and the interested valence band maximum (VBM) and conduction band minimum (CBM) are slightly above the potential barriers between layers, as shown in Fig. 3(a). Then we solve the one-dimensional Schrodinger

TABLE I. Fitted parameters for band gaps, the first optical absorption peak ("optical gap") and exciton binding energy of few-layer black phosphorus according to the formula $A/N^{\alpha} + B$.

	DFT/PBE	GW	Optical gap	Binding energy
α	0.85	0.73	0.96	0.53
A (eV)	0.79	1.70	0.87	0.83
B (eV)	0.04	0.30	0.28	0.03

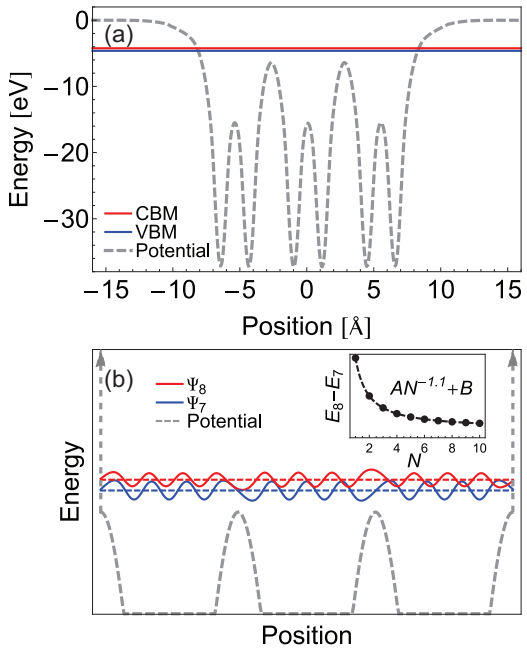

FIG. 3. (Color online) (a) VBM and CBM with Hartree potential obtained from trilayer phosphorene by DFT simulations. (b) Energy levels and wave functions of the seventh and eighth eigenvalues under the infinite quantum well with periodic potential barriers. The inset is the fitting result of the energy spacing between Ψ_7 and Ψ_8 according to the number of periodic potential barriers.

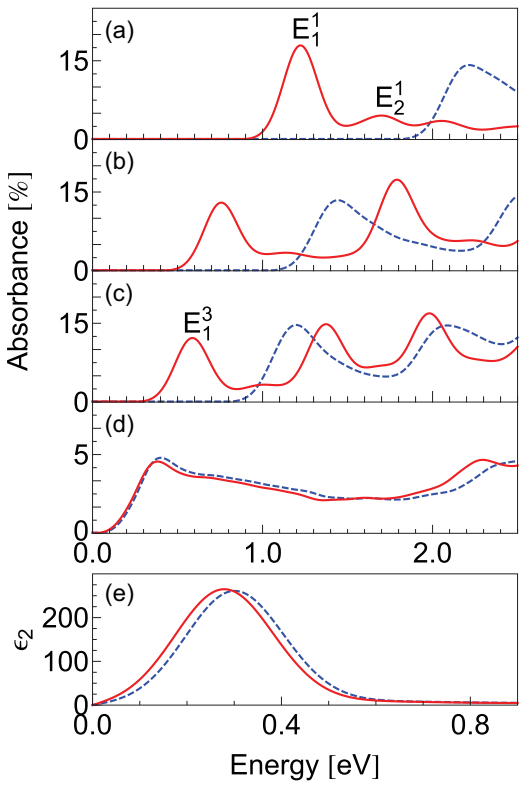

FIG. 4. (Color online) Optical absorption spectra of monolayer (a), bilayer (b), trilayer (c), and bulk phosphorene [(d) and (e)] for the incident light polarized along the x (armchair) direction. In particular, (d) is the optical absorbance per layer in bulk phosphorus. The single-particle optical absorption spectra are presented by dashed lines while those spectra with e-h interaction included are presented by solid lines. We employ a 0.1 eV Gaussian smearing in these plots.

equation in Fig. 3(b) and also focus on energy levels slightly above the potential barriers. By varying the number of periodic barrier potential, the energy spacing between neighboring levels is extracted and their dependence on the width (the number of periodic potential barriers) is concluded in the inset panel of Fig. 3(b). The power law fitting exponent is around 1.1, which is substantially smaller than 2. It is obvious that this fitting value is sensitive to the choices of energy levels. For lower energy levels, this exponent will be smaller; for higher energy levels, this exponent will approach 2. Finally, it is apparent in Table I and Fig. 2 that the optical absorption peaks and exciton binding energies are affected by the same mechanisms; they follow similar scaling laws with the stacking layer number.

IV. EXCITONIC EFFECTS ON OPTICAL ABSORPTION SPECTRA

The optical absorption spectra of monolayer, bilayer, trilayer, and bulk phosphorene structures are presented in Fig. 4 for incident light polarized along the armchair (Γ-X) direction. In all of the studied few-layer structures [Figs. 4(a)–4(c)], excitonic effects substantially reshape optical spectra; all of the main optical features are dominated by excitonic states. For example, in the monolayer structure, the first absorption peak is located at 1.2 eV, which is a strongly bound excitonic state with an 800-meV e-h binding energy. These exciton binding energies in phosphorene are comparable to those found in other monolayer semiconductors and 1D nanostructures [27,31–33]. The reduced dimensionality and depressed screening are primary factors for fostering such enhanced excitonic effects.

Recently, a photoluminescence measurement of monolayer phosphorene was performed [5]. The measured spectral peak position (1.45 eV) is marked in Fig. 2; it resides slightly above our single-shot GW-BSE result. Self-consistently updating the Green's function spectrum and dielectric function using the G_1W_1 methodology yields an exciton energy of 1.4 eV, as shown in Fig. 2. However, self-consistent G_1W_1 may not always give better band gap. More importantly, it should be noted that extrinsic factors may influence experimental data, such as defects and doping [5], which may account for some of the disagreement between experiments and our calculations. Therefore, additional experimental results must be assessed before further conclusions can be made about the necessity of self-consistence.

In the bulk limit of black phosphorus, the optical absorption spectrum is nearly unchanged by the inclusion of e-h interactions [Figs. 4(d) and 4(e)]. Our simulation estimates the upper limit of the exciton binding energy as 30 meV, which is similar to those in other bulk semiconductors [17]. However, this is surprisingly different from similar layered materials. For example, bulk hexagonal BN possesses a significant exciton binding energy of 600 meV [24]. We attribute the small excitonic effects in bulk phosphorous to its stronger interlayer interactions, which is exhibited by its sizable interlayer band dispersion [13], making it a true three-dimensional material

unlike other, more weakly coupled layer structures. We have also compared the electronic charge distributions of monolayer and bulk phosphorene. The interlayer interaction results in the reduction of interlayer distance and substantial out-plane features [34]. This interlayer interaction and the corresponding coupling reduce the perpendicular quantum confinement, resulting in smaller band gaps and weaker excitonic effects.

V. ANISOTROPIC OPTICAL RESPONSE

The optical absorption spectra for light polarized along the zigzag direction of few-layer black phosphorous is presented in Fig. 5. These host profoundly-distinct absorption energy ranges from the armchair spectra; the prominent absorption features begin at higher energies—near 2.8 eV. Thus monolayer phosphorene strongly absorbs armchair-polarized light with energies between 1.1 and 2.8 eV and is transparent to zigzag-polarized light in the same energy range; this phenomenon is the result of selection rules associated with the symmetries of this anisotropic material. Phosphorene is thus a natural optical linear polarizer, which can be used in liquid-crystal displays, three-dimensional visualization techniques, (bio)dermatology, and in optical quantum computers [35,36]. Furthermore, the polarization energy window is tunable through a wide range. Comparing Figs. 4 and 5, the high end of the polarization window is nearly fixed at 2.8 eV, while the low end can be reduced from 1.1 eV down to 300 meV, by adjusting the layer stacking number. This frequency range is very exploitable for applications—it covers the infrared and near-infrared regimes. Finally, this anisotropic optical response can be used to identify the orientations of few-layer black phosphorous in experiments.

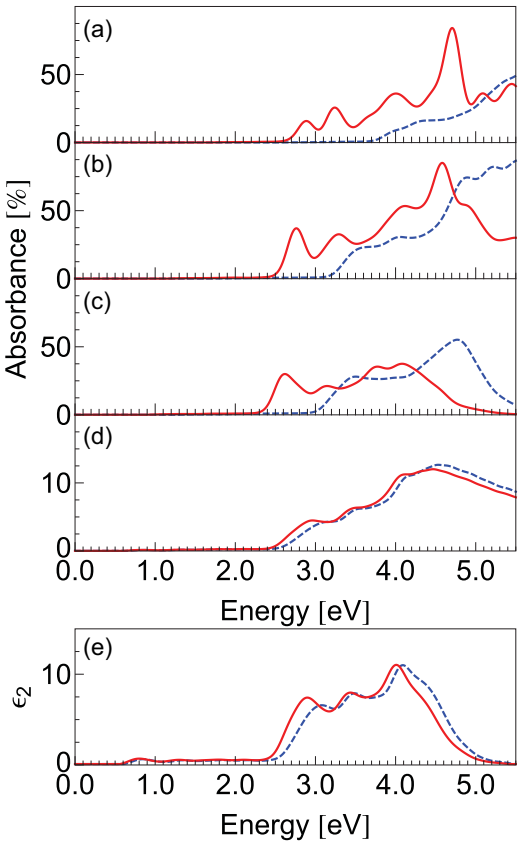

FIG. 5. (Color online) Optical absorption spectra of monolayer (a), bilayer (b), trilayer (c), and bulk phosphorene [(d) and (e)] for the incident light polarized along the y (zigzag) direction. In particular, (d) is the optical absorbance per layer in bulk phosphorus. The single-particle optical absorption are presented by dashed lines while those spectra with e-h interaction included are presented by solid lines.

VI. ANISOTROPIC EXCITONS

We have plotted wave functions of typical bright excitons in Fig. 6. An overall character of these excitons is that their spatial distribution of wave functions is anisotropic and, in particular, is extended along the armchair direction. This is consistent with the anisotropic band dispersion shown in Fig. 1(b). These excitons form striped patterns, similar to those found in bundles of nanowires. This is due to the fact that the near-isotropic binding Coulomb interaction pulls on electrons that are mobile only along one direction. Interestingly, the optical activities of these plotted excitons are strongly correlated with their spacial anisotropy; they are optically bright only for the incident light polarized along the extended direction (armchair direction) of their wave function, if we compare Figs. 4, 5, and 6.

If we compare wave functions of the first two bright excitons [E_1^1 and E_2^1 marked in Fig. 4(a)] from the same series in monolayer phosphorene [Figs. 6(a) and 6(b)], we see that their respective distributions resemble one another both perpendicular to the structure and along the stripe direction (armchair axis). It should be noted that the second excitonic state (E_2^1) has a clear nodal structure perpendicular to the stripe direction (along the zigzag axis), though one expects a 1D exciton to exhibit nodes along the stripe direction. The wave function of the first bright exciton (E_1^3) of trilayer phosphorene is plotted in Figs. 6(c) and 6(e). Although the hole is fixed in one layer, electrons are distributed on both layers. Thus the spatial extent of, and the interactions between, the excitons can also be controlled by the layer stacking number.

VII. IMPACTS OF INTERLAYER DISTANCE

Finally, we assess the dependence of the many-electron effects on the interlayer distance and dimensionality. Our studies show that the interlayer distance slightly changes from bilayer to bulk black phosphorus (less than 0.8%). Meanwhile, QP band gaps and intralayer excitons of suspended few-layer phosphorene (which is treated with a Coulomb truncation) are not very sensitive to the change of interlayer distances. For example, the band gap of bilayer phosphorene varies by less than 60 meV for the change of interlayer distance of ± 0.5 Å. These many-electron effects are rooted in the vast vacuum that surrounds the isolated system, and are consequently not significantly affected by small changes of the interlayer distance. The layers of bulk black phosphorous, on the other hand, do not interface with a vacuum, and their excited state properties are sensitive to the interlayer distance. A small change of ± 0.5 Å in the interlayer distance can shift the band gap and exciton energy by 150 meV, which is significant by comparison to the 300-meV band gap [34]. Obviously, if the

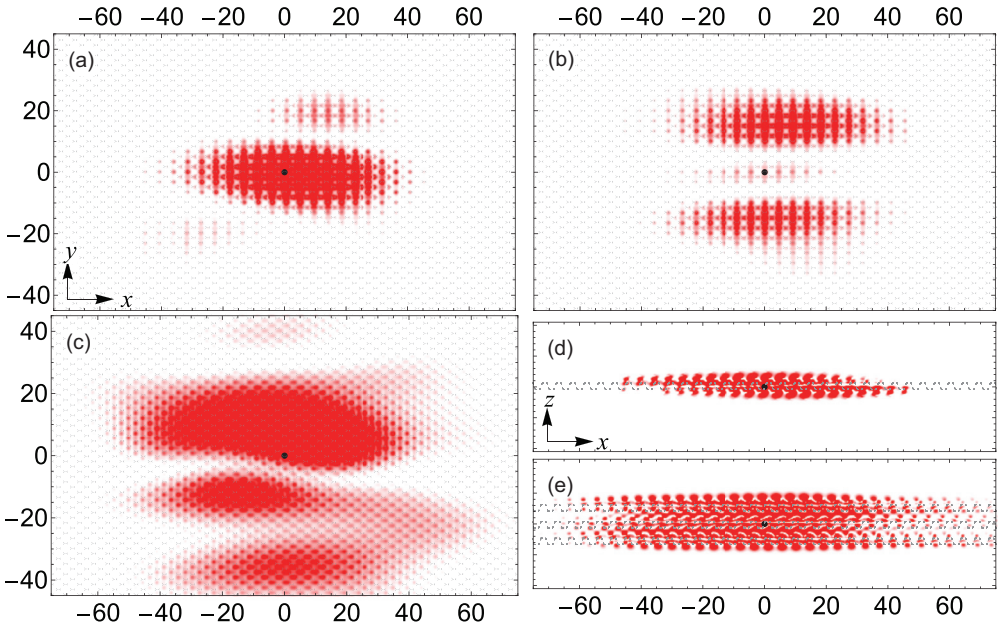

FIG. 6. (Color online) (a), (b) Top views of the square of the electron wave functions of the first and second bound excitons in monolayer phosphorene [marked as E_1^1 and E_2^1 in Fig. 4(a)]. (c) Top view of the electron wave function of the first bound exciton in trilayer phosphorene [marked as E_1^3 in Fig. 3(c)]. (d), (e) Side view of the wave functions in (a) and (c), respectively. The hole, represented by a black dot, is fixed at the origin. Lines representing the atomic bonds are superimposed. The scale is in angstroms.

thickness of few-layer black phosphorus is larger than the characteristic size of QPs or excitons, many-electron effects shall smoothly evolve to the bulk limit. Based on sizes of excitons plotted in Fig. 6, we estimate the critical thickness is around 10 nm, which is roughly around 20 layers.

VIII. SUMMARY

In conclusion, first-principles simulations have been performed to determine the defining properties of few-layer black phosphorus and their exciting potential applications. Enhanced many-electron effects are essential in shaping their band gaps and optical responses because of anisotropic band dispersions and the effectively quasi-1D nature. In particular, our discovered uniquely anisotropic optical response with *e-h* interactions included makes phosphorene ideal for linear optical polarizers, covering the infrared and a part of the visible light regime of broad interest. Finally, we show that all these properties can be efficiently tuned by the stacking layer number, which is potentially useful for device design.

ACKNOWLEDGMENTS

We are supported by NSF Grant No. DMR-1207141. We acknowledge Erik Henriksen and Ruixiang Fei for fruitful discussions. The computational resources have been provided by Lonestar of Teragrid at the Texas Advanced Computing Center. The ground state calculation is performed by QUANTUM ESPRESSO [37]. The GW-BSE calculation is done with the BERKELEYGW package [38].

[1] K. S. Novoselov, A. K. Geim, S. V. Morozov, D. Jiang, Y. Zhang, S. V. Dubonos, I. V. Grigorieva, and A. A. Firsov, Science **306**, 666 (2004).
[2] A. K. Geim and K. S. Novoselov, Nat. Mater. **6**, 183 (2007).
[3] A. H. Castro Neto, F. Guinea, N. M. R. Peres, K. S. Novoselov, and A. K. Geim, Rev. Mod. Phys. **81**, 109 (2009).
[4] Likai Li, Yijun Yu, Guo Jun Ye, Qingqin Ge, Xuedong Ou, Hua Wu, Donglai Feng, Xian Hui Chen, and Yuanbo Zhang, Nat. Nanotechnol. **9**, 372 (2014).
[5] Han Liu, Adam T. Neal, Zhen Zhu, Zhe Luo, Xianfan Xu, David Tománek, and Peide D. Ye, ACS Nano **8**, 4033 (2014).
[6] Fengnian Xia, Han Wang, and Yichen Jia, arXiv:1402.0270.
[7] Eugenie Samuel Reich, Nature (London) **506**, 19 (2014).
[8] Jingsi Qiao, Xianghua Kong, Zhi-Xin Hu, Feng Yang, and Wei Ji, arXiv:1401.5045.
[9] A. Splendiani, L. Sun, Y. Zhang, T. Li, J. Kim, C. Y. Chim, G. Galli, and F. Wang, Nano Lett. **10**, 1271 (2010).
[10] Sefaattin Tongay, Jian Zhou, Can Ataca, Kelvin Lo, Tyler S. Matthews, Jingbo Li, Jeffrey C. Grossman, and Junqiao Wu, Nano Lett. **12**, 5576 (2012).
[11] C. Ataca, H. Sahin, and S. Ciraci, J. Phys. Chem. C **116**, 8983 (2012).
[12] Allan Brown and Stig Rundqvist, Acta Cryst. **19**, 684 (1965).
[13] Y. Takao, H. Asahina, and A. Morita, J. Phys. Soc. Jpn. **50**, 3362 (1981).
[14] John P. Perdew, Kieron Burke, and Matthias Ernzerhof, Phys. Rev. Lett. **77**, 3865 (1996).
[15] N. Troullier and J. L. Martins, Phys. Rev. B **43**, 1993 (1991).
[16] M. S. Hybertsen and S. G. Louie, Phys. Rev. B **34**, 5390 (1986).
[17] M. Rohlfing and S. G. Louie, Phys. Rev. B **62**, 4927 (2000).

[18] S. Ismail-Beigi, Phys. Rev. B **73**, 233103 (2006).
[19] C. A. Rozzi, D. Varsano, A. Marini, E. K. U. Gross, and A. Rubio, Phys. Rev. B **73**, 205119 (2006).
[20] C. D. Spataru, S. Ismail-Beigi, L. X. Benedict, and S. G. Louie, Appl. Phys. A: Mater. Sci. Process. **78**, 1129 (2004).
[21] L. Yang, C. D. Spataru, S. G. Louie, and M. Y. Chou, Phys. Rev. B **75**, 201304 (2007).
[22] B. Radisavljevic, A. Radenovic, J. Brivio, V. Giacometti, and A. Kis, Nat. Nanotechnol. **6**, 147 (2011).
[23] Saptarshi Das, Hong-Yan Chen, Ashish Verma Penumatcha, and Joerg Appenzeller, Nano Lett. **13**, 100 (2013).
[24] Ludger Wirtz, Andrea Marini, and Angel Rubio, Phys. Rev. Lett. **96**, 126104 (2006).
[25] B. Arnaud, S. Lebègue, P. Rabiller, and M. Alouani, Phys. Rev. Lett. **96**, 026402 (2006).
[26] A. Ramasubramaniam, Phys. Rev. B **86**, 115409 (2012).
[27] Diana Y. Qiu, Felipe H. da Jornada, and Steven G. Louie, Phys. Rev. Lett. **111**, 216805 (2013).
[28] R. Soklaski, Y. Liang, and L. Yang, Appl. Phys. Lett. **104**, 193110 (2014).
[29] Robert W. Keyes, Phys. Rev. **92**, 580 (1953).
[30] Douglas Warschauer, J. Appl. Phys. **34**, 1853 (1963).
[31] L. Yang, M. L. Cohen, and S. G. Louie, Nano Lett. **7**, 3112 (2007).
[32] C. D. Spataru, S. Ismail-Beigi, L. X. Benedict, and S. G. Louie, Phys. Rev. Lett. **92**, 077402 (2004).
[33] F. Wang, G. Dukovic, L. E. Brus, and T. F. Heinz, Science **308**, 838 (2005).
[34] See Supplemental Material at http://link.aps.org/supplemental/10.1103/PhysRevB.89.235319 for the impact of the interlayer distance on band gaps and a detailed discussion of interlayer distance on the band gap of bulk black phosphorus.
[35] N. Zeng, X. Jiang, Q. Gao, Y. He, and H. Ma, Appl. Opt. **48**, 6734 (2009).
[36] A. Knill, R. Laflamme, G. J. Milburn, Nature (London) **409**, 46 (2001).
[37] P. Giannozzi, S. Baroni, N. Bonini, M. Calandra, R. Car, C. Cavazzoni, D. Ceresoli, G. L. Chiarotti, M. Cococcioni, I. Dabo, A. Dal Corso, S. Fabris, G. Fratesi, S. de Gironcoli, R. Gebauer, U. Gerstmann, C. Gougoussis, A. Kokalj, M. Lazzeri, L. Martin-Samos, N. Marzari, F. Mauri, R. Mazzarello, S. Paolini, A. Pasquarello, L. Paulatto, C. Sbraccia, S. Scandolo, G. Sclauzero, A. P. Seitsonen, A. Smogunov, P. Umari, and R. M. Wentzcovitch, J. Phys.: Condens. Matter **21**, 395502 (2009).
[38] Jack Deslippe, Georgy Samsonidze, David A. Strubbe, Manish Jain, Marvin L. Cohen, and Steven G. Louie, Comput. Phys. Commun. **183**, 1269 (2012).